THE JOURNAL OF PHYSICAL CHEMISTRY B

Article

pubs.acs.org/JPCB

Morphologies near Cloud Point in Aqueous Ionic Surfactant: Scattering and NMR Studies

Sanjeev Kumar,*[,†] Arti Bhadoria,[†] Harsha Patel,[†] and Vinod K. Aswal[‡]

[†]Soft Material Research Laboratory, Department of Chemistry, The Maharaja Sayajirao University of Baroda, Vadodara, 390 002 Gujarat, India

[‡]Solid State Physics Division, Bhabha Atomic Research Centre, Trombay, Mumbai 400 085, India

ABSTRACT: Clouding phenomenon in ionic surfactant solution is fairly a new addition to the conventional phenomenon observed with nonionic counterpart. Various scattering and spectroscopic techniques, dynamic light scattering (DLS), small angle neutron scattering (SANS), and nuclear magnetic resonance (NMR), have been used to draw information regarding the aggregate morphologies (formed by an ionic surfactant, tetra-*n*-butylammonium dodecylsulphate, TBADS) when the surfactant solution passes through the cloud point (CP). DLS measurements have shown that two morphologies are present when the system approaches the CP. The data revealed that individual micelles (~5 nm) convert to giant aggregates (~500 nm) over the range of temperature including the CP. SANS experiments have been performed to draw the information regarding individual micellar fraction below and above the CP. NMR spectra at different temperatures have been collected for TBADS solution. The broadening and the downfield shift of $-N-CH_2$ and $-O-CH_2$ proton peaks support the micellar growth as the sample was heated. The above peaks show splitting (into two each) confirming the presence of two morphologies around the CP. It is noted that conversion of only a small fraction of individual micelles is responsible for the clouding.

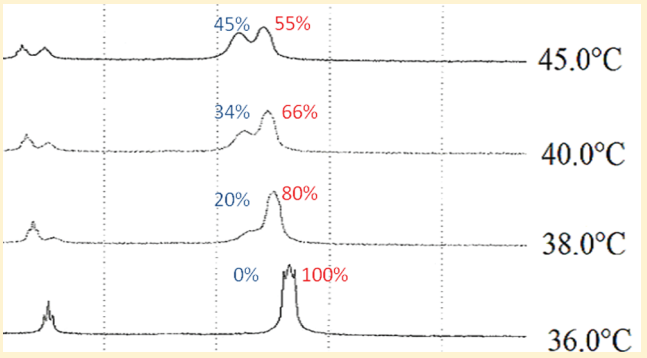

INTRODUCTION

Recent developments in the description of interaction of charged colloidal particles with short-range attractive forces have led to the interesting findings including metastable liquid−liquid phase separation and the formation of dynamically arrested morphologies (such as attractive and repulsive glasses and transient gels.[1−3] A number of globular proteins have analogies with colloids/surfactant micelles that interact via a short-range attractive force.

The interfacial water in the immediate vicinity of hydrophobic and hydrophilic surfaces plays a predominant role in various phenomena like folding and activity of proteins and clouding/phase separation in surfactant and polymer solutions, among others.[4−9] There are two types of surfactant (ionic and nonionic); the solution behavior with influence of temperature on each type are in sharp contrast. Nonionic surfactant solutions (e.g., CiEj type) cannot withstand elevated temperature and undergo clouding followed by phase separation into surfactant lean and surfactant rich phases at a well-defined temperature known as cloud point (CP or T_{CP}).[10] In the past, it was assumed that clouding and phase separation is not possible in aqueous ionic surfactant solutions due to electrostatic repulsion between the charged micelles, but recent studies have demonstrated that the phenomenon can be observed in ionic surfactant solutions with and without salt.[11−20] A number of applications are reported for the CP phenomenon in diverse fields,[21−24] but the mechanism by which it occurs is not yet clear and still a source of controversy among different groups.[13,14,16,20,25,26] The Langer−Schwartz theory[27] predicts that the nucleated phase may appear as a cloud of small droplets that grow slowly beyond the critical droplet size or that it may form as an isolated droplet that rapidly grows to a very large size. The analogy can be drawn to surfactant solution in which liquid−liquid immiscibility occurs above lower critical solution temperature (LCST) or CP. Using a lattice gas theory, it has been shown that CP arises from a sudden increase in rotational entropy caused by rapid breaking of H-bonds between water and surfactant heads.[25] In ionic surfactant solutions, above bonds are expected even stronger due to ion-dipole interactions. In recent reports, it has been proposed that the formation of the connected micellar network[28] or strongly orientation dependent interactions[21] between water and micellar head groups could be responsible for the clouding phenomenon.

Most of the studies on the clouding behavior in charged micellar systems were made where tetra-*n*-butyl ammonium counterion (TBA^+) was added either externally or was a part of the anionic surfactant monomer species.[11,12,15,19] Also, the

Received: January 18, 2012
Revised: February 28, 2012
Published: February 29, 2012

   dx.doi.org/10.1021/jp300630w | *J. Phys. Chem. B* 2012, 116, 3699−3703

change in headgroup from tripropyl to tributyl ammonium in a cationic surfactant causes the appearance of clouding on heating.[29] In spite of various intelligent prepositions, no experimental evidence is available regarding the morphology of micelles when the system approaches the CP. Keeping this view in mind, various studies (DLS, NMR, and SANS) are performed to collect the evidence regarding the micellar morphologies (as well as their fractions) in anionic surfactant solution (tetra-*n*-butylammonium dodecylsulphate, TBADS) near the CP. This work may find application in stimuli sensitive phenomenon in amphiphilic systems, in protein folding/unfolding, and in the field of thermo responsive formulations.

EXPERIMENTAL SECTION

Materials. Sodium dodecyl sulfate, SDS (≥99%), and tetrabutylammonium bromide, TBAB (99%) were purchased from Sigma St Louis, USA. TBADS has been prepared by mixing equimolar solutions of TBAB and SDS followed by extraction with dichloromethane. The purity of the TBADS was confirmed by ^{1}H NMR, IR, mass spectroscopy, and surface tensiometry. The critical micelle concentration (cmc) and other spectroscopic data of TBADS were in agreement with those reported earlier.[16] All the inorganic salts (ammonium bromide (NH_4Br), sodium bromide (NaBr), lithium bromide (LiBr), and cesium bromide (CsBr)) were of highest purity grade available and used as received. D_2O used for sample preparation was the same as used earlier.[17] The water used to prepare the sample solutions was double distilled in an all-glass distillation apparatus. The specific conductivity of the water was in the range $2-4 \times 10^{-6}$ S·cm^{-1}.

Experiments. The CP values were obtained by placing sample tubes, containing surfactant solution with a fixed concentration of salt or no salt, into a temperature-controlled water bath. The onset of turbidity (visual observation) was taken as the CP. Similar CP measurements were also made by diluting the samples with stock surfactant solutions in order to collect CP data at various concentrations of salt. The uncertainty in the measured CP was ±0.1 °C.

DLS measurements were performed using a Malvern 4800 Autosizer employing a 7132 digital correlator. The light source was Ar-ion laser operated at 514.5 nm with a maximum power output of 2 W. The sample was filtered through 0.2 mm filters (Millipore) to avoid interference from dust particles.

SANS measurements were carried out using a SANS diffractometer at Dhruva Reactor, Trombay, India.[30] The mean wavelength of the neutrons used was 5.2 Å. The samples were placed in a quartz sample holder of thickness 2 mm with the varying temperature below and above CP. The measured SANS data have been corrected and normalized to an absolute scale using standard procedure.[18,31] In SANS measurements, one measures the differential scattering cross-section per unit volume ($d\Sigma/d\Omega$) as a function of scattering vector $Q = 4\pi \sin\theta/\lambda$, where 2θ is the scattering angle, and λ is the wavelength of incident radiation, and for monodisperse micelle solution, it can be expressed as[32]

$$d\Sigma/d\Omega = n_m V_m^2(\rho_m - \rho_s)^2\{\langle F^2(Q)\rangle + \langle F(Q)\rangle^2 [S(Q) - 1]\} + B \quad (1)$$

Where n_m and V_m are the number density and volume of micelles, respectively, $F(Q)$ is the single particle form factor that depends upon shape and size of particles, $S(Q)$ is the interparticle structure factor, and B denotes the incoherent scattering contributed from hydrogen in the micelle. The detailed analysis and relevant expressions are similar as reported earlier.[17,18]

^{1}H NMR spectra were obtained with a Bruker Avance 500 Spectrometer at different temperatures (25−50 °C). The TBADS solution was prepared in D_2O. About 1 mL of solution was transferred to a 5 mm NMR tube and chemical shifts were recorded on the δ (ppm) scale.

RESULTS AND DISCUSSION

Below the CP, surfactant dissolves in water, and at/or above CP the nonionic surfactant solution separates into two isotropic liquid phases; one is a diluted surfactant solution, and the other is a surfactant rich phase. The phase volume and distributed [surfactant] ratio in the two phases can be very high in such systems.[33] TBADS solution shows clouding (and phase separation) on heating in a similar manner as nonionic surfactants. It is interesting to note that in the charged micellar solution, the surfactant goes slowly in giant aggregates with increase in temperature beyond CP. Even at CP, the so-called surfactant lean phase has sufficient fraction of individual micelles observed by phase volume changes and concentration determination by tensiometry; the 0.1 M TBADS solution on heating gives 0.023 M in the lean phase on separation at CP. Subsequently, we detected by visual observation that a turbid system on standing at CP, the phase separates into two clear phases, which on further heating gets cloudy again. The volume of one phase increases at the cost of the other on standing at a temperature beyond CP. In the present study, we employ a combination of different methods such as visual observation, CP, DLS, NMR, and SANS measurements to ascertain the morphology of aggregates. The data demonstrate that a gradual conversion of individual micellar fraction into the giant aggregates takes place as the temperature approaches the CP and even beyond CP. We show that micellar fraction can be tuned by [TBADS], temperature, [salt], and also by the nature of the salt.

Different models have been employed to provide a mechanism of clouding, but nearly all of them are mere speculations.[10,34,35] The picture is even more hazy regarding the mechanism of CP phenomenon in charged micellar solutions.[16,36,37] TBADS solution contains anionic micelles and a TBA^+ counterion. It has been proposed by Vlachy et al.[38] that the organic counterion should strongly interact with the soft sulfate headgroup resulting in a fairly strong ion-pair close to an uncharged dipolar headgroup. Further TBA^+ would like to stay near the micellar headgroup region also because of hydrophobic interactions. As a result, the formation of hydrophobic aggregates is expected, which do not dissolve in the bulk solution. The aggregate may phase separate with the removal of water molecules still sticking to the aggregate surface. The increase in temperature may cause the removal of above sticked water of micellar surface and play a role in the appearance of clouding. On the basis of the above discussion, it is expected that all four butyl chains of TBA^+ would like to go toward the micellar core, but this may cause a gauche conformation.[18,39] A plausible explanation is the assumption that the two butyl chains would stay toward the micellar core, and the remaining two toward the bulk water.[40] The latter butyl chains may link micelles together. However, all micelles are not expected to involve in the process of linking and can be the cause of formation of two different morphologies near CP though they are formed by the same precursors. This probably is the reason

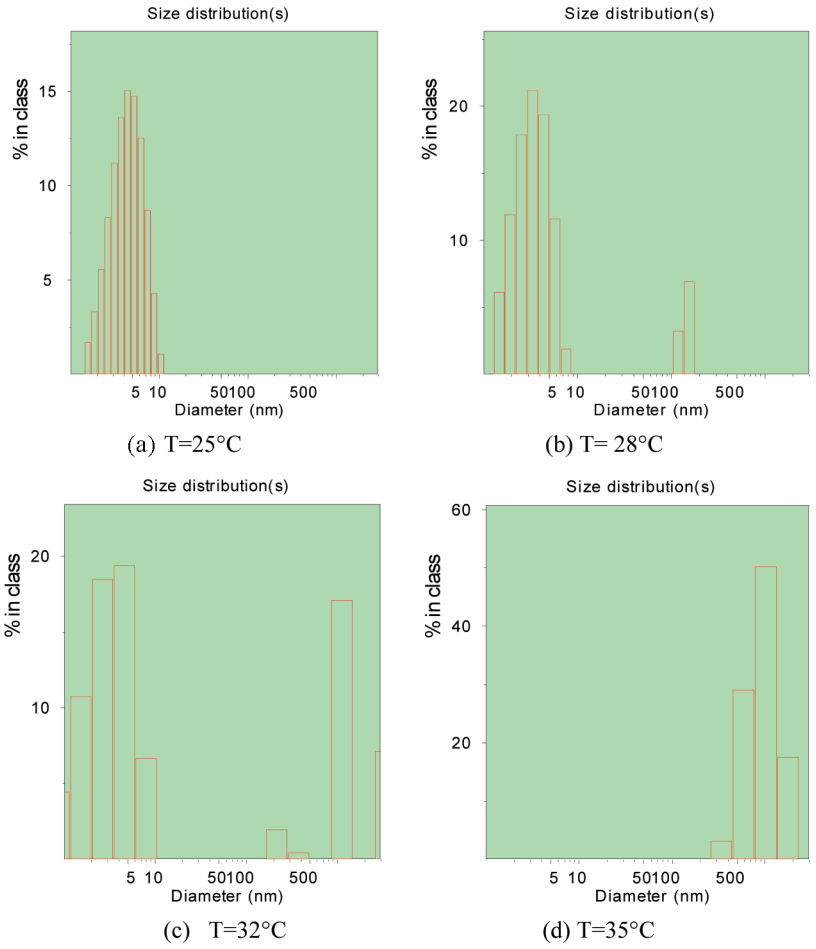

Figure 1. DLS data at different temperatures below (a and b), near (c), and above CP (d) of 0.1 M TBADS (CP = 31.5 °C).

that only a small fraction of giant aggregate is sufficient to produce clouding in the solution. It has been proposed that stearic restrictions would not allow all the dissociated TBA^+ to house in the volume available at the micellar surface.[16] Therefore, few TBA^+ could be available in the bulk aqueous phase. At low $[TBA^+]$ in the bulk water, the entropy of mixing of such TBA^+ throughout bulk phase overwhelms the finite driving force to assemble, making aggregates no more than metastable. The idea of the formation of giant aggregates in the presence of TBA^+ may find support from the fact that surfactant parameter[41] ($P = v/a_h l$, where v and l are the volume and lengh of the alkyl part, respectively, and a_h is the headgroup area) increases in the presence of various counterions due to a decrease in the value of a_h. The formation of various surfactant microstructures (e.g., rod-like micelles, vesicles, lamellar phase, and precipates) in aqueous salt solutions has been observed and explained in the light of increase in P.[42−44]

The TBA^+ of the bulk phase may have a tendency to interact with water facing butyl chains of micelle bound TBA^+. However, micelle bound TBA^+ may be comparatively in a more favorable environment than the one present in bulk water. The giant aggregates are caused by micelle linking, which can be understood in terms of the dependence of hydrophobic solvation on solute size (e.g., butyl chains). Near ambient conditions, the driving force will get stronger with increasing temperature. This could be the reason of clouding in charged micellar solutions discussed above. For emulsions, Jansson et al.[45] argued that attractive hydrophobic interactions between the droplets are facilitated with the adsorption of such hydrophobic counterions. With the increase of temperature, the entropy cost of ordering water around such butyl chains of bulk TBA^+ becomes untenable. The resulting energetic effect due to the loss of hydrogen bonding derives the removal of a more hydrophobic entity (giant aggregates) from water.[46] The discussion finds support from the fact that clouding behavior in an ionic micellar solution appears mostly where TBA^+ was added either externally or was part of the surfactant monomer. It has been seen earlier that less tetra-*n*-pentyl ammonium bromide is required to show more clouding than tetra-*n*-butyl ammonium bromide when present with SDS.[47] Therefore, symmetrical organic counterions seems to be the major driving force for a soft surfactant headgroup such as sulfate or sulfonate.[38] In few studies, various morphologies (uni- and multilamellar vesicles, flat aggregates, or bilayer fragment)[42,44,48] were assigned for the giant aggregates. In view of the complex situation, more work is required for the complete understanding of the morphologies formed by the tetra alkyl ammonium surfactants with another combination of soft cations and soft head groups.

To corroborate the above proposition, DLS measurements have been performed. DLS data at different temperatures, below and above the CP, have shown the development of bigger morphologies at the cost of smaller ones in addition to smaller ones even below CP (Figure 1). This suggests that two types of morphologies are present when the system is about to reach CP.

dx.doi.org/10.1021/jp300630w | J. Phys. Chem. B 2012, 116, 3699−3703

Because of the bigger size of the giant aggregate, it is expected to be invisible by SANS experiment (beyond the detection limit of SANS spectrometer).[49] If only giant aggregates are present near CP, we would have only measured the background from the sample (i.e., bulk phase). The scattering from the individual micelles exist at CP and even beyond CP (Figure 2). The scattering intensity gradually

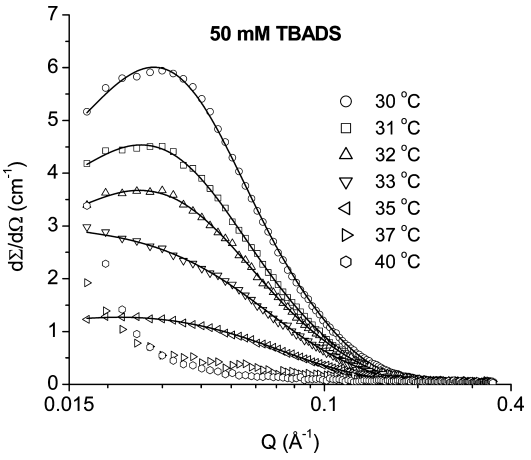

Figure 2. SANS data on 0.05 M TBADS at different temperatures.

Table 1. Micellar Parameters of 0.05 M TBADS with Varying Temperature

temp (°C)	semiminor axis $b = c$ (Å)	semimajor axis a (Å)	aggregation number N	fractional charge α	individual micellar fraction (%)
30	18.9	79.7	195	0.03	100
31	18.8	69.4	168	0.03	78
32	17.9	64.4	141	0.03	70
33	17.7	51.8	110	0.01	52
35	17.0	47.6	93	0.01	30

decreases with an increase in temperature above CP. Tables 1 and 2 show that individual micellar volume fraction decreases as

Table 2. Micellar Parameters of 0.02 M TBADS with Varying Temperature

temp (°C)	semiminor axis $b = c$ (Å)	semimajor axis a (Å)	aggregation number N	fractional charge α	individual micellar fraction (%)
30	17.2	48.1	99	0.06	100
32	17.2	49.6	102	0.06	100
34	17.4	48.3	101	0.05	94
36	17.2	43.2	87	0.04	80
38	17.2	38.7	78	0.03	63
40	16.7	37.8	71	0.01	48

temperature passes the CP. The rate of conversion of individual micelle to giant aggregates on heating seems dependent upon the initial concentration of TBADS. For 0.05 M TBADS (CP = 31.5 °C), 22% of the micellar fraction already converted into giant aggregates. However, for 0.02 M TBADS, the fraction was ~6% at its CP (34 °C).

It was interesting to note that the fraction of individual micelles or giant aggregates can be tuned by the presence of inorganic salts taken in by the system (Table 3). At 30 °C, the addition of NH_4Br to 0.03 M TBADS has no effect on the

Table 3. Micellar Fraction and CP (in D_2O) of 0.03 M TBADS with Different Salts

		individual micellar fraction (%)	
0.03 M TBADS + salt	CP (°C)	30 °C	45 °C
no salt	33.2	100	21
0.01 M NH_4Br	33.8	100	
0.03 M NH_4Br	37.3	100	
0.05 M NH_4Br	40.9	100	44
0.06 M NaBr	39.5	100	79
0.06 M LiBr	38.5	100	62
0.06 M CsBr	36.0	100	90

individual micellar fraction (i.e., 100%). It could be understood in the light of the fact that 0.03 M TBADS has CP at 33.2 °C and 100% of the individual micelles are present at 31 °C (<CP). In an earlier study, it has been shown that CP increases with the addition of inorganic salts (NaBr, CsBr, and LiBr).[19] Therefore, when the system is far from CP, the whole micellar volume is present as individual micelles (Table 3). This may be due to the fact that the exchange of bigger TBA^+ (less hydrated) with smaller inorganic counterions (more hydrated) can take place resulting in increased water near the micellar surface, and hence, CP of the system would go higher (Table 3), and the possible linking of micelles is less favored (at low [inorganic salt]). Also, this indicates that the giant aggregates present in the systems (at 45 °C) can be transformed back in to individual micelles with the addition of inorganic salts (e.g., CsBr). Again, softness of counterions from Li^+ to TBA^+ and their partitioning near themicellar headgroup region have a role to decide the final morphologies and clouding behavior of the resulting system.[38] This indeed was observed from our SANS studies.

The collected data show that the micelles just below CP start linking with the difference (for the case of nonionic surfactant) that a significant amount of the surfactant remained in the form of individual micelles. The individual charged micelles convert to giant aggregates gradually near and beyond the CP.

The ^1H NMR spectroscopy is found to be the most convenient method for the monitoring of changes in aggregate morphology. The spectra of TBADS in D_2O at different temperatures are collected. The observed chemical shifts (δ) are comparable with the reported values.[36] NMR data show the shifting of spectra as a whole to higher δ (ppm) scale (downfield) together with broadening of a few peaks as the temperature increases. This shows the dehydration of TBA^+ and micellar headgroup region as the temperature increases together with the micellar growth[50] favoring the formation of two morphologies near CP (Figure 3). The decrease in electron density around the proton is supported by deshielding with the increase in temperature. The higher δ value also corroborates the increase in attractive forces resulting in clustering of micelles or giant aggregates. The $-N-CH_2$ proton peak of TBA^+ at 3.2 and $-O-CH_2$ peak of DS^- at 3.95 shows the gradual splitting into two separate peaks due to the alteration of the chemical environment experienced by the above two protons (Figure 3). The NMR study indicates that the above two protons are distributed into two different morphologies (individual micelles and giant aggregates).

dx.doi.org/10.1021/jp300630w | J. Phys. Chem. B 2012, 116, 3699−3703

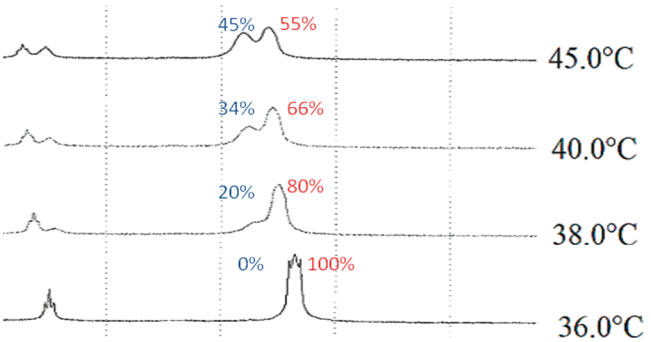

Figure 3. ^{1}H NMR spectra (500 MHz) for $-O-CH_2$ and $-N-CH_2$ protons in TBADS solution at different temperatures showing the percent of two morphologies (individual micelle, %, and giant aggregate, %) just below and above the CP (38 °C).

CONCLUSIONS

The study allows us to conclude that conversion of individual micelles to giant aggregate may be the reason of clouding specifically in ionic surfactant solution (e.g., TBADS). The process is observed more gradually than that in nonionic surfactant solutions. This may be due to the presence of charged micelles in the former case. For clouding, only a small fraction of individual micelles is needed that convert into giant aggregates. It appears that a cloud of small micelles grows slowly beyond the critical size and forms the basis of the clouding phenomenon.[27] The percent of giant aggregates/micelle can be tuned by the [TBADS], temperature, [salt], and even by nature of the salt.

AUTHOR INFORMATION

Corresponding Author

*E-mail: drksanjeev@gmail.com.

Notes

The authors declare no competing financial interest.

ACKNOWLEDGMENTS

We acknowledge the UGC–DAE CSR (CRS-151) for the financial support. We also thank Dr. P. A. Hassan, Chemistry Division, BARC, Trombay, Mumbai, India, for instrumental support of the Dynamic Light Scattering.

REFERENCES

(1) Trappe, V.; Prasad, V.; Cipelletti, L.; Segre, P. N.; Weitz, D. A. *Nature* **2001**, *411*, 772–775.
(2) Pham, K. N.; Puertas, A. M.; Bergenholtz, J.; Egelhaaf, S. U.; Moussaid, A.; Pusey, P. N.; Schofield, A. B.; Cates, M. E.; Fuchs, M.; Poon, W. C. K. *Science* **2002**, *296*, 104–106.
(3) Eckert, T.; Bartsch, E. *Phys. Rev. Lett.* **2002**, *89*, 125701–125704.
(4) Chandler, D. *Nature* **2005**, *437*, 640–647.
(5) Tanford, C. *Science* **1978**, *200*, 1012–1018.
(6) Kauzmann, W. *Adv. Protein Chem.* **1959**, *14*, 1–63.
(7) Sreejith, L.; Parathakkat, S.; Nair, S. M.; Kumar, S.; Hassan, P.; Talmon, Y.; Verma, G. *J. Phys. Chem. B* **2011**, *115*, 464–470.
(8) Peleshanko, S.; Anderson, K. D.; Goodman, M.; Determan, M. D.; Mallapragada, S. K.; Tsukruk, V. T. *Langmuir* **2007**, *23*, 25–30.
(9) Narayanan, J.; Deotare, V. W. *Phys. Rev. E* **1999**, *60*, 4597–4603.
(10) Dong, R.; Hao, J. *Chem. Rev.* **2010**, *110*, 4978–5022.
(11) Kumar, S.; Aswal, V. K.; Naqvi, A. Z.; Goyal, P. S.; Kabir-ud-Din. *Langmuir* **2001**, *17*, 2549–2550.
(12) Yu, Z. J.; Xu, G. *J. Phys. Chem.* **1989**, *93*, 7441–7445.
(13) Raghavan, S. R.; Edlund, H.; Kaler, E. W. *Langmuir* **2002**, *18*, 1056–1064.
(14) Yan, Y.; Li, L.; Hofffmann, H. *J. Phys. Chem. B* **2006**, *110*, 1949–1954.
(15) Zana, R.; Benrraou, M.; Bales, B. L. *J. Phys. Chem. B* **2004**, *108*, 18195–18203.
(16) Bales, B. L.; Zana, R. *Langmuir* **2004**, *20*, 1579–1581.
(17) Kabir-ud-Din.; Sharma, D.; Khan, Z. A.; Aswal, V. K.; Kumar, S. *J. Colloid Interface Sci.* **2006**, *302*, 315–321.
(18) Aswal, V. K.; Kohlbrecher, J. *Chem. Phys. Lett.* **2006**, *424*, 91–96.
(19) Ahmad, T.; Kumar, S.; Khan, Z. A.; Kabir-ud-Din. *Colloids Surf., A* **2007**, *294*, 130–136.
(20) Mukherjee, P.; Padhan, S. K.; Dash, S.; Patel, S.; Mishra, B. K. *Adv. Colloid Interface Sci.* **2011**, *162*, 59–79.
(21) Quina, F. H.; Hinze, W. L. *Ind. Eng. Chem. Res.* **1999**, *38*, 4150–4168.
(22) Madej, K. *Trends Anal. Chem.* **2009**, *28*, 436–446.
(23) Materna, K.; Goralska, E.; Sobczynska, A.; Szymanowski, J. *Green Chem.* **2004**, *6*, 176–182.
(24) Sahin, C. A.; Efecinar, M.; Satiroglu, N. *J. Hazard. Mater.* **2010**, *176*, 672–677.
(25) Bock, H.; Gubbins, K. E. *Phys. Rev. Lett.* **2004**, *92*, 135701–135704.
(26) Kalur, G. C.; Raghavan, S. R. *J. Phys. Chem. B* **2005**, *109*, 8599–8604.
(27) Langer, S.; Schwartz, A. J. *Phys. Rev. A* **1980**, *21*, 948–958.
(28) Zilman, A.; Safran, S. A.; Sottmann, T.; Strey, R. *Langmuir* **2004**, *20*, 2199–2207.
(29) Buckingham, S. A.; Garvery, C. J.; Warr, G. G. *J. Phys. Chem.* **1993**, *97*, 10236–10244.
(30) Aswal, V. K.; Goyal, P. S. *Curr. Sci.* **2000**, *79*, 947–953.
(31) Hayter, J. B.; Penfold, J. *Colloid Polym. Sci.* **1983**, *261*, 1022–1030.
(32) Chen, S. H.; Lin, T. L. In *Methods of Experimental Physics*; Price, D. L., Skold, K., Eds.; Academic Press: New York, 1987; Vol. *23*, p 489.
(33) Wei, Q.; Yan, H.; Yuwen, D.; Youyuan, D. *Chin. J. Chem. Eng.* **2008**, *16*, 722–725.
(34) Tasaki, K. *J. Am. Chem. Soc.* **1996**, *118*, 8459–8469.
(35) Valkenburg, B. V.; Wang, X.; Damath, J. *Science* **2004**, *306*, 101–104.
(36) Mitra, D.; Chakraborty, I.; Bhattacharya, S. C.; Moulik, S. P. *Langmuir* **2007**, *23*, 3049–3061.
(37) Rout, D. K.; Chauhan, S.; Agarwal, A. *Ind. Eng. Chem. Res.* **2009**, *48*, 8842–8847.
(38) Vlachy, N.; Jagoda, B. C.; Vacha, R.; Touraud, D.; Jungwirth, P.; Kunz, W. *Adv. Colloid Interface Sci.* **2009**, *146*, 42–47.
(39) Kumar, S.; Sharma, D.; Kabir-ud-Din. *Langmuir* **2000**, *16*, 6821–6824.
(40) Almgren, M.; Swarup, S. *J. Phys. Chem.* **1983**, *87*, 876–881.
(41) Israelachvili, J. N.; Mitchell, D. J.; Ninham, B. W. *J. Chem. Soc., Faraday Trans. 2* **1976**, *72*, 1525–1568.
(42) Sein, A.; Engberts, J. B. F. N. *Langmuir* **1995**, *11*, 455–465.
(43) Raghavan, S. R.; Kaler, E. W. *Langmuir* **2001**, *17*, 300–306.
(44) Vlachy, N.; Renoncourt, A.; Drechsler, M.; Verbavatz, J. M.; Touraud, D.; Kunz, W. *J. Colloid Interface Sci.* **2008**, *320*, 360–363.
(45) Jansson, M.; Eriksson, L.; Skagerlind, P. *Colloids Surf.* **1991**, *53*, 157–167.
(46) Chandler, D. *Nature* **2002**, *417*, 491–491.
(47) Kumar, S.; Sharma, D.; Kabir-ud-Din. *Langmuir* **2003**, *19*, 3539–3541.
(48) Porte, G. *J. Phys. Chem.* **1983**, *87*, 3541–3550.
(49) Goyal, P. S.; Menon, S. V. G.; Dasanacharya, B. A.; Thiyagarajan, P. *Phys. Rev. E* **1995**, *51*, 2308–2315.
(50) Siddiqui, U. S.; Khan, F.; Khan, I. A.; Dar, A. A.; Kabir-ud-Din. *J. Colloid Interface Sci.* **2011**, *355*, 131–139.